longer tie-line length, with exceptions occurring in the region close to the critical point.

The phase-composition data from Tables I-V are plotted in phase diagrams in Figures 1-5, respectively. The tie lines are determined by connecting each corresponding set of total, bottom, and top phase points. The binodial curve is drawn through the top and bottom phase points, and is estimated near the critical point on the basis of the locations and trends of the top and bottom phase compositions and, in some cases, single phase points.

The phase diagrams with $(NH_4)_2SO_4$, $MgSO_4$, or Na_2SO_4 combined with PEG 1000 or PEG 8000 were determined using the HPLC method. The remainder of the diagrams were determined gravimetrically. Points from the HPLC data sets were repeated using the gravimetric method. While both methods had virtually the same reproducibility and resulted in values identical within their uncertainty, the gravimetric technique was simpler and less labor intensive.

Literature Cited

(1) Albertsson, P.-A. *Partition of Cell Particles and Macromolecules*, 3rd ed.; Wiley-Interscience: New York, 1986.
(2) Walter, H.; Brooks, D. E.; Fisher, D. *Partitioning in Aqueous Two-Phase Systems*; Academic Press, Inc.: Orlando, FL, 1985.
(3) Cabezas, H., Jr.; Kabiri-Badr, M.; Szlag, D. C. *Bioseparation* **1990**, *1*, 227.
(4) Edmond, E.; Ogston, A. G. *Biochem. J.* **1968**, *109*, 569.
(5) King, R. S.; Blanch, H. W.; Prausnitz, J. M. *AIChE J.* **1988**, *34*, 1585.
(6) Kabiri-Badr, M. Ph.D. Thesis, University of Arizona, Tucson, AZ, 1990.
(7) Szlag, D. C.; Guiliano, K. A.; Snyder, S. M. In *Downstream Processing and Bioseparation*; Hamel, J.-F. P., Hunter, J. B., Sikdar, S. K., Eds.; ACS Symposium Series 419; American Chemical Society: Washington, DC, 1990; pp 71-86.
(8) Diamond, A. D.; Hsu, J. T.; *Biotechnol. Bioeng.* **1989**, *34*, 1000.
(9) Stewart, R.; Todd, P. In *Proceedings from Frontiers in Bioprocessing II*; Sikdar, S., Todd, P., Bier, M., Eds.; ACS Symposium Series; American Chemical Society: Washington, DC, in press.

Received for review July 26, 1991. Revised January 10, 1992. Accepted January 28, 1992.

Anion Exchange in Amberlite IRA-400 and Amberlite IRA-410 Ion Exchange Resins

Modesto López, José Coca, and Herminio Sastre*

Department of Chemical Engineering, University of Oviedo, 33071 Oviedo, Spain

Equilibrium for the binary exchange of anions on Amberlite IRA-400 and Amberlite IRA-410 was measured. Standard methods were used to determine operating characteristics of both resins. Equilibrium data were obtained by the batch method. The fitting of binary ion exchange isotherm equations is an important aspect of data analysis. The Langmuir, Freundlich, Slips, and Koble-Corrigan isotherms were transformed to a linear form and their adjustable parameters estimated by linear regression. The Langmuir isotherm is the most suitable for both correlation of equilibrium data and prediction and interpretation of *breakthrough curves*.

Introduction

The three factors that can affect the behavior of an ion exchange column are *equilibrium*, *kinetics*, and *mechanics*. The degree of column efficiency depends primarily on equilibrium (*1*, *2*).

Various methods have been used to obtain binary ion-exchange equilibrium data. The simplest is the *batch method*, proposed by Gregor and Bergman (*3*).

The dimensionless *equivalent ionic fraction*, x and y, for fluid and solid, respectively, are defined by

$$x = C_i/C_0 \qquad y = Q_i/Q$$

where C_i = concentration of the ion species in the solution, C_0 = total concentration of the solution phase, Q_i = concentration of the ion species in the solution phase, and Q = total exchange capacity of the resin.

* To whom correspondance should be addressed.

This paper focuses on the study of the anion equilibrium data of the Amberlite IRA-400 and IRA-410 resins fitted to linear transformations of different isotherm equations. The regression coefficients for each resin were determined.

Experimental Section

The resin phase consisted of Amberlite IRA-400 (type I) and Amberlite IRA-410 (type II) gel strong-base anion exchange resins (supplied by Rohm and Haas Co.) in the X-form (X = CO_3H, Cl, OH, SO_4). Solution phases were mixtures made up using sodium salts of both the X-anion and fluoride anion required to obtain a total concentration of 0.05 N.

The resins were *washed* with distilled deionized water and *regenerated or eluted* with 4% sodium sulfate, except in elutions of sulfate ion where 1 N sodium nitrate was used (*4*).

The resins were conditioned by alternate conversions to the hydroxide and chloride forms and washed until no further chloride could be detected in the effluent. Part of this material was converted into the bicarbonate, chloride, hydroxide, and sulfate forms.

To determine the *water content* of the wet resin, resin samples were put in a Büchner funnel which was connected to a water vacuum pump to remove the interstitial water. After weighing, the resin samples were dried in a desiccator over phosphorus pentoxide to constant weight. The *resin density* was determined in water by a standard-type picnometer. The *total capacity* for weighed amounts (approximately 5 g) of the ionic form of the resin was determined by adding an excess of sodium salt of X-anions, washing until no further X-anion could be detected in the effluent, regenerating the resin with exactly 1 L each of 4% sodium sulfate (or 1 N sodium nitrate), collecting this effluent in a volumetric flask, and finally determining the X-anion (*5*-*8*). Table I shows the physicochemical characteristics of the used resins.

In the *batch equilibrium studies*, weighed amounts (2-3 g) of moist resin were equilibrated with 100 mL of mixtures of

0021-9568/92/1737-0274$03.00/0

Table I. Physicochemical Parameters of the Resins Used

parameter	Amberlite IRA-400					Amberlite IRA-410				
	F^-	OH^-	Cl^-	CO_3H^-	SO_4^{2-}	F^-	OH^-	Cl^-	CO_3H^-	SO_4^{2-}
true density/(g/mL)	1.09	1.08	1.09	1.11	1.12	1.10	1.08	1.12	1.15	1.15
apparent density/(g/mL)	0.73	0.73	0.73	0.74	0.75	0.73	0.73	0.71	0.73	0.76
humidity/%	52.5	58.1	47.4	49.0	47.7	46.5	52.4	40.8	40.8	43.4
ion-exchange capacity/(mequiv/g)	1.42	1.46	2.0	1.89	1.79	1.82	1.78	2.19	2.06	1.90

Table II. Equilibrium Data for the Ion-Exchange Equilibrium

$$R_zX + F \rightleftharpoons zRF + X$$

$$X = OH, CO_3H, Cl, SO_4 \quad z = 1, 2$$

bicarbonate form				chloride form			
IRA-400		IRA-410		IRA-400		IRA-410	
x	y	x	y	x	y	x	y
0.1049	0.0196	0.2189	0.0783	0.0967	0.0117	0.1011	0.0199
0.2118	0.0427	0.3263	0.0995	0.1889	0.0260	0.2086	0.0360
0.3138	0.0633	0.4252	0.1383	0.2911	0.0380	0.3022	0.0556
0.4089	0.1027	0.5258	0.2018	0.3904	0.0584	0.4087	0.0745
0.5038	0.1424	0.6247	0.2661	0.4894	0.0795	0.5145	0.1073
0.6012	0.1924	0.7137	0.3511	0.5897	0.1125	0.5916	0.1406
0.6945	0.2510	0.8155	0.4829	0.6883	0.1515	0.6975	0.2148
0.7959	0.353	0.8853	0.6308	0.7876	0.2164	0.7932	0.2943
0.8977	0.5230	0.9324	0.7235	0.8801	0.3288	0.8816	0.4099
0.9422	0.6354			0.9267	0.4156	0.9319	0.5293
0.9462	0.6519			0.9566	0.5040	0.9528	0.6161
hydroxide form				sulfate form			
IRA-400		IRA-410		IRA-400		IRA-410	
x	y	x	y	x	y	x	y
0.0963	0.1268	0.1972	0.0816	0.2342	0.0179	0.2333	0.0227
0.1969	0.2514	0.3002	0.1240	0.4765	0.0662	0.4785	0.0731
0.2934	0.3659	0.3982	0.1693	0.7183	0.1720	0.7243	0.1740
0.3868	0.4636	0.4850	0.2265	0.8570	0.3477	0.8605	0.3043
0.4845	0.5618	0.5962	0.2782	0.8893	0.3545	0.8929	0.3493
0.5833	0.6653	0.6925	0.3578	0.9077	0.3630	0.9003	0.4012
0.6751	0.7142	0.7849	0.4427	0.9227	0.4036	0.9227	0.4121
0.7660	0.7681	0.8913	0.6049	0.9380	0.4555	0.9457	0.4609
0.8590	0.8673						
0.9078	0.8953						
0.9407	0.8990						

exchanging ions at a total concentration of 0.5 N. The mixture was equilibrated at room temperature (19 ± 1 °C) in stoppered bottles with intermittent shaking. Resin samples were separated from the solution by a funnel supported in a 250-mL volumetric flask.

Fluoride ion was determined in each phase by a fluoride-selective electrode (*9*).

Results and Discussion

Table II presents the equilibrium results for all presaturant ions as the equivalent ionic fraction. These results were fitted to various isotherm equations. Although the best model is not necessarily that which gives the best fit, in the present work four linear isotherm equations (*10*) were considered and a mathematic comparison of the suitability of the fit was made. These equations (*11*) are given in Table III.

The Langmuir (L) and Freundlich (F) isotherms contain one adjustable parameter while the Slips (S) and Koble–Corrigan (K–C) isotherms contain two adjustable parameters. The Slips and Koble–Corrigan isotherms reduce to the Langmuir isotherm when their exponents are set to unity.

Table III lists dimensionless isotherm equations and linear transformations used for fitting by the linear regression method. The values of adjustable parameters and linear regression coefficients are summarized in Tables IV (Amberlite IRA-400) and V (Amberlite IRA-410).

Figures 1 and 2 show that experimental results can be described in all cases by the Slips and Koble–Corrigan isotherms. They offer more flexibility than the Langmuir and Freundlich isotherms.

From a statistic point of view, all the transformations of the isotherm equations listed in Table II tend to low weight y values more than high y values. This is a consequence of the linear transformation.

As can see in Figures 1 and 2, for general purposes, the Langmuir isotherm seems more suitable for describing ion exchange studied in both Amberlite IRA-400 and Amberlite IRA-410 than the Freundlich isotherm. In this case, r is not a suitable criterion of the goodness of fit, because y deviations are measured in ln y–ln x space.

Conclusions

Although the use of a second adjustable parameter improves the fit obtained by means of the Langmuir isotherm, the only parameter of this equation, the *separation factor* (*12*), is the most valuable design parameter in column performance, and the fit by linear regression supplies the appropriate parameter. The Freundlich isotherm reveals important systematic deviations from results. The Slips and Koble–Corrigan isotherms introduce a second parameter, in most cases, with negligible improvement in goodness of fit.

The result in the present study lead to the following conclusions: (1) The data were successfully correlated with the Langmuir isotherm. (2) The fit by linear regression gives the separation factor. (3) The Langmuir isotherm is the most suitable for both data prediction and correlation.

Table III. Isotherm Equations and Their Linear Transformations

	isotherm equation	linear transformation
Langmuir (L)	$y = \frac{x}{a + (1 - a)x}$	$x/y = a + (1 - a)x$
Freundlich (F)	$y = x^n$	$\ln y = n \ln x$
Slips (S)	$y = \left[\frac{x}{b + (1 - b)}\right]^s$	$x/y^{1/s} = b + (1 - b)x$
Koble–Corrigan (K–C)	$y = \frac{x^t}{c + (1 - c)x^t}$	$x^t/y = c + (1 - c)x^t$

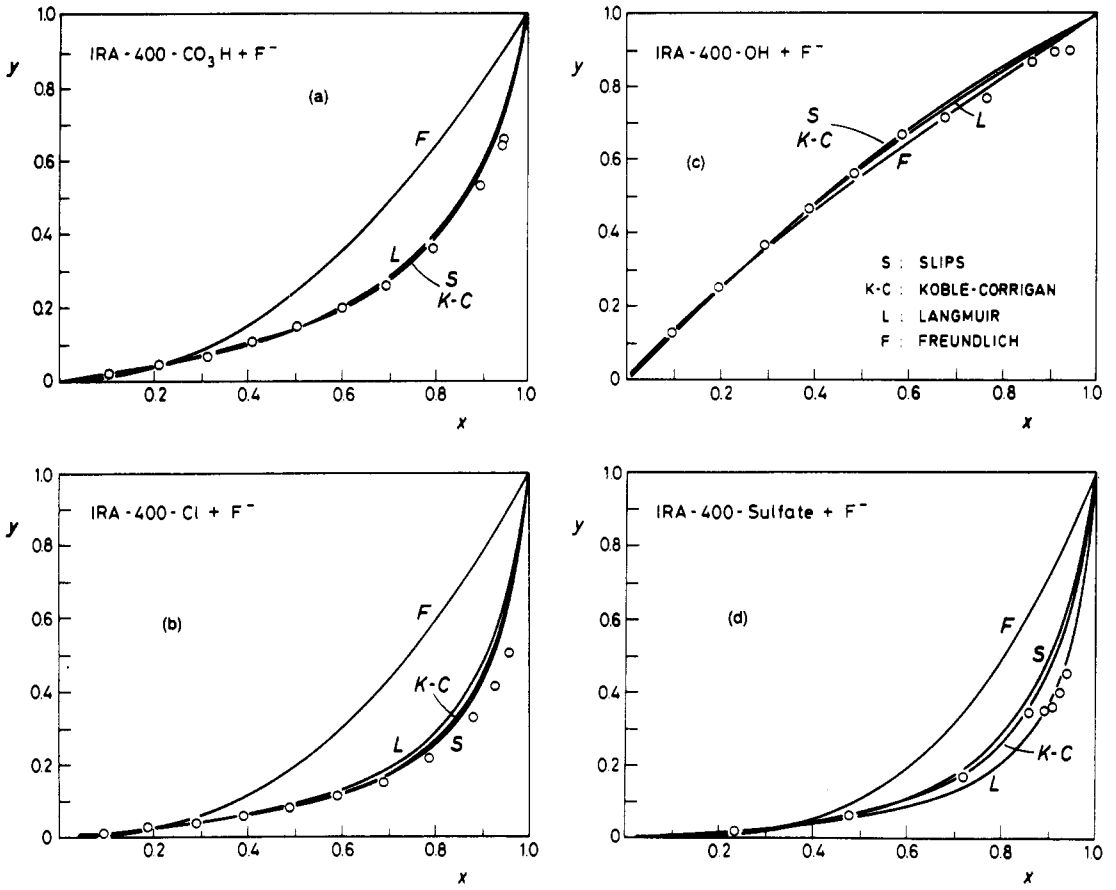

Figure 1. Ion-exchange isotherms for fluoride ions on Amberlite IRA-400: experimental results and correlation models. X: (a) CO_3H, (b) Cl, (c) OH, (d) sulfate.

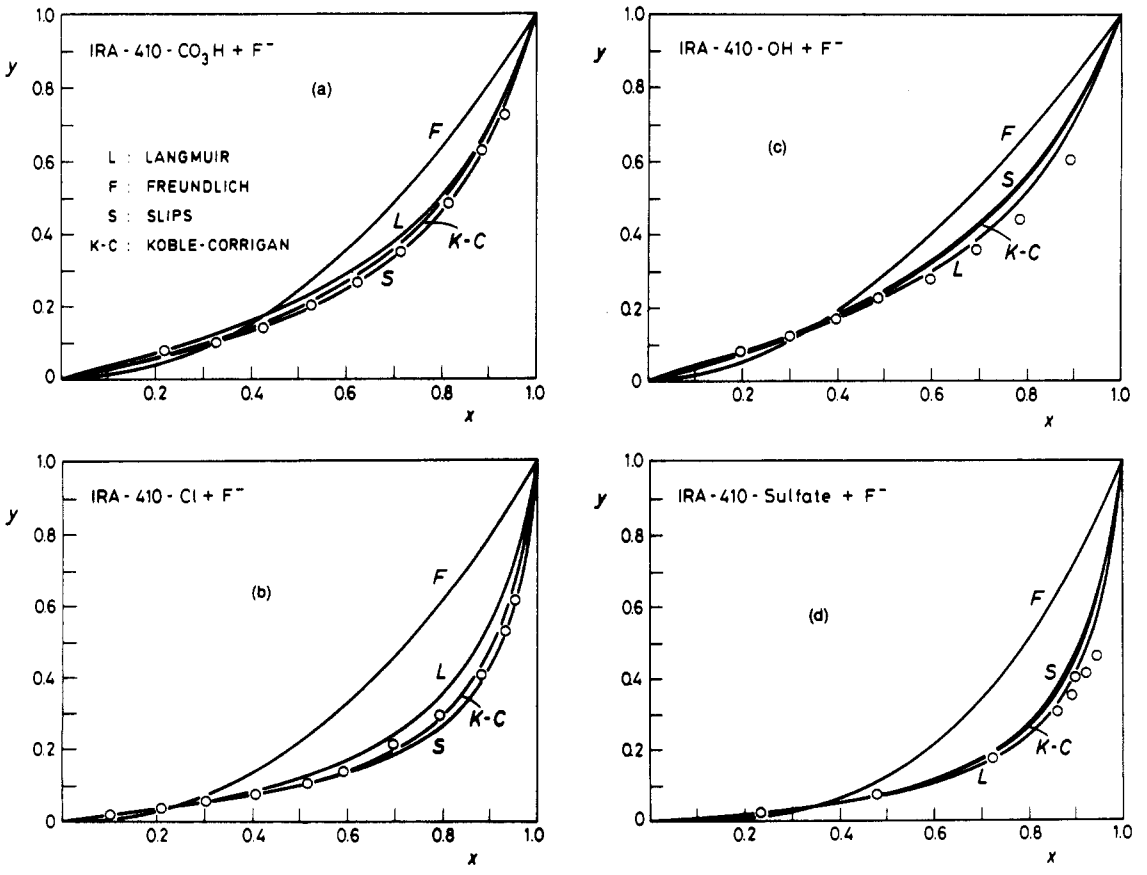

Figure 2. Ion-exchange isotherms for fluoride ions on Amberlite IRA-410: experimental results and correlation models. X: (a) CO_3H, (b) Cl, (c) OH, (d) sulfate.

Table IV. Parameters and Linear Regression Coefficients in Amberlite IRA-400

equation	param	value for different ionic forms: bicarbonate	chloride	hydroxide	sulfate
Langmuir	a	6.19	9.91	0.74	15.20
	r	0.9942	0.9859	0.9865	0.9812
Freundlich	n	2.08	2.36	0.86	3.17
	r	0.9804	0.9714	0.9977	0.9925
Slips	b	7.03	13.99	0.58	6.15
	s	0.96	0.91	1.16	1.34
	r	0.9953	0.9952	0.9961	0.9974
Koble–Corrigan	c	7.07	13.29	0.62	6.75
	t	0.93	0.85	1.10	1.55
	r	0.9959	0.9954	0.9952	0.9957

Table V. Parameters and Linear Regression Coefficients in Amberlite IRA-410

equation	param	value for different ionic forms: bicarbonate	chloride	hydroxide	sulfate
Langmuir	a	4.11	7.22	3.17	12.74
	r	0.9395	0.9419	0.9591	0.9949
Freundlich	n	2.03	2.16	1.78	3.02
	r	0.9745	0.9622	0.9912	0.9883
Slips	b	4.48	18.41	3.26	8.54
	s	0.90	0.77	0.96	1.14
	r	0.9988	0.9954	0.9822	0.9989
Koble–Corrigan	c	5.15	17.21	5.44	8.67
	t	0.91	0.59	0.70	1.25
	r	0.9986	0.9986	0.9968	0.9988

Glossary

a	separation factor, dimensionless
b	Slips isotherm parameter, dimensionless
c	Koble–Corrigan isotherm parameter, dimensionless
C_l	concentration of the anion in the solution phase, equiv/L
C_0	total concentration of the solution phase, equiv/L
Q	total exchange capacity of the resin, equiv/L
Q_l	concentration of the anion in the solution phase, equiv/L
n	Freundlich isotherm parameter, dimensionless
R	resin matrix
s	Slips isotherm parameter, dimensionless
t	Koble–Corrigan isotherm parameter, dimensionless
x	equivalent ionic fraction in solution phase, dimensionless
y	equivalent ionic fraction in resin phase, dimensionless
z	absolute values of the ionic valence

Registry No. F^-, 16984-48-8; OH^-, 14280-30-9; HCO_3^-, 71-52-3; Cl^-, 16887-00-6; SO_4^{2-}, 14808-79-8; Amberlite IRA 400, 9002-24-8; Amberlite IRA 410, 9002-26-0.

Literature Cited

(1) Rodrigues, A. E. *NATO ASI Ser., Ser. E* **1981**, *33*, 35.
(2) Schweitzer, P. A. *Handbook of separation techniques for chemical engineers*; McGraw-Hill: New York, 1979; Section 1.12, pp 1-383.
(3) Turner, J. C. R.; Murphy, T. K. *Chem. Eng. Sci.* **1983**, *38*, 147.
(4) López, M. Doctoral Thesis, Universidad de Oviedo, Oviedo, Spain, 1989.
(5) Fisher, S.; Kunin, R. *Anal. Chem.* **1955**, *27*, 1191.
(6) Gregor, H. P.; Held, K. M.; Bellin, J. *Anal. Chem.* **1951**, *23*, 620.
(7) Helfferich, F. *Ion exchange*; McGraw-Hill: New York, 1962; p 90.
(8) *AMBERLITE ion exchange resins laboratory guide*; Rohm and Haas: Philadelphia.
(9) Clesceri, L. S., Greenberg, A. E., Trussell, R. R., Eds. *Standard Methods for the Examination of Water and Wastewater*, 17th ed.; American Health Association: Washington, DC, 1989.
(10) Kinniburg, D. G. *Environ. Sci. Technol.* **1986**, *20*, 895.
(11) Perry, R. H.; Chilton, C. H. *Chemical engineers' handbook*, 4th ed.; McGraw-Hill: Tokyo, 1963; Section 16, pp 18-8.
(12) Clifford, D. A. Ph.D. Thesis, University of Michigan, Ann Arbor, MI, 1976.

Received for review August 5, 1991. Accepted December 17, 1991.

Liquid–Liquid Equilibria for Quaternary Systems Containing Methanol, Alkane, and Aromatic Compounds

Hideki Higashiuchi, Yujiro Sakuragi, Masanori Nagatani,† and Yasuhiko Arai*

Department of Industrial Chemistry, Kurume College of Technology, Kurume 830, Japan

The mutual solubilities and tie-line data for type I quaternary systems heptane + methanol + benzene + toluene and octane + methanol + benzene + toluene and for type II quaternary systems heptane + methanol + benzene + octane and heptane + methanol + *p*-xylene + octane were measured at 25 °C. The experimental results have been successfully correlated using an improved Wilson equation.

Introduction

There have been few measurements on the liquid–liquid equilibrium for quaternary systems (*1*). In earlier papers (*2*, *3*), mutual solubilities and tie-line data were reported for several binary and ternary systems containing alkane, methanol, and

* Address correspondence to Y.A., Department of Chemical Engineering, Faculty of Engineering, Kyushu University, Fukuoka 812, Japan.
† Present address: Department of Chemical Engineering, Faculty of Engineering, Fukuoka University, Fukuoka 814-01, Japan.

Table I. Type I and Type II Quaternary Systems

no.	type	system
1	I	heptane (1) + methanol (2) + benzene (3) + toluene (4)
2	I	octane (1) + methanol (2) + benzene (3) + toluene (4)
3	II	heptane (1) + methanol (2) + benzene (3) + octane (4)
4	II	heptane (1) + methanol (2) + *p*-xylene (3) + octane (4)

Table II. Solubility Data for Heptane (1) + Methanol (2) + Benzene (3) + Toluene (4) at 25 °C

x_1	x_2	x_3	x_4
	R_1 (0.75 Benzene + 0.25 Toluene)		
0.6659	0.2219	0.0841	0.0281
0.4320	0.4288	0.1043	0.0349
0.2285	0.6821	0.0665	0.0229
	R_2 (0.50 Benzene + 0.50 Toluene)		
0.6619	0.2320	0.0489	0.0572
0.4312	0.4264	0.0657	0.0767
0.2337	0.6915	0.0345	0.0403
	R_3 (0.25 Benzene + 0.75 Toluene)		
0.6636	0.2331	0.0256	0.0777
0.4222	0.4284	0.0370	0.1124
0.2255	0.6870	0.0216	0.0659

0021-9568/92/1737-0277$03.00/0